10 kV, 39 mΩ·cm^2 Multi-Channel AlGaN/GaN Schottky Barrier Diodes

Ming Xiao, Yunwei Ma, Kai Liu, Kai Cheng, and Yuhao Zhang, *Member, IEEE*

***Abstract*—This work demonstrates multi-channel AlGaN/GaN Schottky barrier diodes (SBDs) with a breakdown voltage (*BV*) over 10 kV, the highest *BV* reported in GaN devices to date. The epitaxial structure consists of a p-GaN cap layer and five AlGaN/GaN channels continuously grown on a low-cost 4-inch sapphire substrate. A novel device design is proposed for electric field management, i.e., the p-GaN reduced surface field (RESURF) structure, which balances the net charges in the multi-channel at reverse biases. The SBD with a 98-µm anode-to-cathode length (L_{AC}) shows a *BV* of 9.15 kV and a specific on-resistance (R_{ON}) of 29.5 mΩ·cm^2, rendering a Baliga's figure of merit (FOM) of 2.84 GW/cm^2. The SBD with a 123-µm L_{AC} shows a *BV* over 10 kV and a R_{ON} of 39 mΩ·cm^2, which is 2.5-fold lower than the R_{ON} of the state-of-the-art 10-kV SiC junction barrier Schottky (JBS) diodes. The Baliga's FOMs of our 4.6-10 kV GaN SBDs well exceed the SiC unipolar limit. These results show the great promise of GaN for medium- and high-voltage power electronics.**

***Index Terms*— gallium nitride, power electronics, p-GaN, Schottky barrier diodes, multi-channel, RESURF, high voltage.**

I. Introduction

High-voltage (HV, >1.7 kV) power rectifiers are needed in various power electronics applications, e.g., renewable-energy generation, industrial motor drives, electricity grid, and transportations. Bipolar Si diodes are commercially available up to 6.5 kV, but they suffer from slow switching speed. Unipolar SiC junction barrier Schottky (JBS) diodes up to 10 kV have been recently pre-commercialized by Cree [1]. However, commercial 3.3-kV+ SiC diodes are barely available due to high cost; their market penetration is still slow.

GaN has superior physical properties over Si/SiC for power applications. Lateral GaN HEMTs have been commercialized up to 650 V. Extensive research is ongoing to push GaN towards HV ranges in both vertical and lateral devices. Vertical GaN p-n diodes up to 5 kV [2], Schottky barrier diodes (SBDs) up to 2 kV [3], and transistors up to 2 kV [4]–[6] have been demonstrated. Lateral GaN SBDs up to 9 kV [7], [8] have been reported based on a single [7] or double [8] two-dimensional-electron (2DEG) channels. Whereas their specific on-resistance ($R_{ON,SP}$) are larger than the similarly-rated SiC JBS diodes.

Recently, the multi-channel lateral GaN device was proposed as a promising candidate for HV devices [9], as it retains a low 2DEG sheet resistance (R_{SH}) while leveraging the benefits of vertical devices, e.g., spatially-distributed current and E-field.

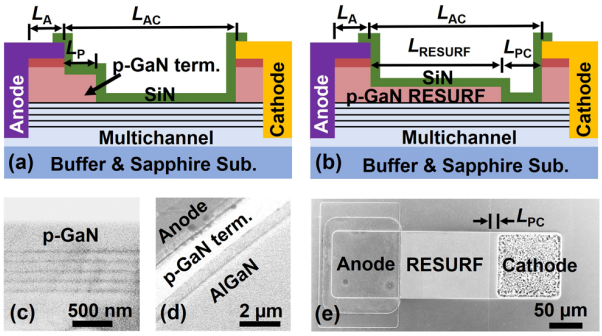

Fig. 1. Schematics of the multi-channel AlGaN/GaN SBD with (a) p-GaN edge termination and (b) p-GaN RESURF. (b) Cross-sectional SEM images of the p-GaN/multi-channel region. (c) SEM image of the p-GaN edge termination region. (d) Top-view SEM image of the multi-channel SBD with p-GaN RESURF (L_{AC} = 123 µm) before SiN_x passivation.

Multi-channel GaN tri-gate SBDs and HEMTs [10], [11] were reported with a breakdown voltage (*BV*) of 0.9-1.2 kV. A planar p-GaN termination was introduced for E-field management, allowing a *BV* over 3.3 kV [9]. Very recently, a 3-D termination with p-n junctions wrapping around multi-2DEG fins enabled a 5.2 kV, 13 mΩ·cm^2 GaN SBD, which shows a Baliga's figure of merit (FOM) exceeding the SiC unipolar limit [12].

This work explores the further *BV* upscaling in multi-channel GaN SBDs and demonstrates the highest *BV* (>10-kV) in GaN devices to date. Our device features a new design for E-field management in multi-channel devices, i.e., the p-GaN reduced surface field (RESURF) structure (Fig. 1). This structure differs from the prior p-GaN termination [9], [12] in that (a) the p-GaN layer extends to near the cathode and (b) the charge balance is newly introduced between the multi-channel and p-GaN. It also differs from the single-channel p-GaN/AlGaN/GaN charge-balanced SBD [13]: in our device, a portion of p-GaN is fully etched to avoid the potential p-GaN punch-through issue, while p-GaN is connected between anode and cathode in [13]. Finally, when compared to the polarization superjunction (PSJ) device [8], our device employs multiple 2DEG channels and an p-GaN RESURF layer. The multi-channel is key to enabling a $R_{ON,SP}$ much lower than that of similarly-rated SiC JBS diodes.

II. Device Fabrication

The wafer in this work consists of 20-nm p^+-GaN ([Mg] ~ 2×10^{19} cm^{-3}), 350-nm p-GaN ([Mg] ~ 4×10^{18} cm^{-3}), five $Al_{0.25}Ga_{0.75}N$ (23 nm)/i-GaN (100 nm) heterostructure channels, and a buffer layer, all continuously grown on a 4-inch sapphire

This work is in part supported by the National Science Foundation under Grant ECCS-2036740 and the CPES Power Management Industry Consortium at Virginia Polytechnic Institute and State University. (*Corresponding Author: Yuhao Zhang*).

M. Xiao, Y. Ma, and Y. Zhang are with the Center of Power Electronics Systems, Virginia Polytechnic Institute and State University, Blacksburg, VA 24060 USA (e-mail: yhzhang@vt.edu).

K. Liu and K. Cheng are with Enkris Semiconductor Inc., Suzhou 215123, China.

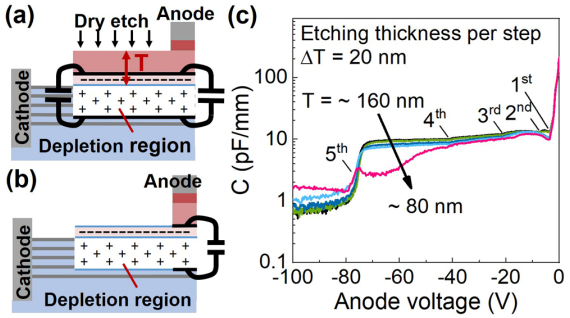

Fig. 2. Diagrams of charges and capacitances (a) before and (b) after reaching the critical p-GaN thickness. (c) C-V characteristics of the test structure along with p-GaN etch. The depletion of each 2DEG channel is marked.

substrate by metal-organic chemical vapor deposition. This continuous growth obviates the need for p-GaN regrowth in [9], [12]. Hall measurements of the entire epi reveal a R_{SH} of 178 Ω/sq, a 2DEG mobility (μ_{2DEG}) of 2010 cm^2/V·s, and a five-channel total 2DEG density (n_{2DEG}) of 1.75×10^{13} cm^{-2}. Note that this n_{2DEG} has accounted the p-GaN depletion effect.

The device fabrication started from a self-aligned Ohmic process for cathode formation similar to the one reported in [9]. A bi-layer resist was used to enable the deep etch and metal lift-off in a single lithography step. A Ti/Al/Ni/Au metal stack was used for the Ohmic formation. After a 900-nm-deep mesa isolation, the anode Schottky contact (Ni/Au) was formed on the mesa to access all 2DEG channels and on top of p-GaN with an extension length (L_A) of 2 µm.

The p-GaN dry etch was then performed. In the reference sample with a p-GaN termination (Fig. 1(a)), the p-termination length (L_P) is 2 µm. Other p-GaN regions between anode and cathode was fully etched. In the p-GaN RESURF sample (Fig. 1(b)), p-GaN was etched blanketly until reaching a critical thickness (T_0) when the charges of remaining p-GaN balance the net charges in the multi-channel. Subsequently, the p-GaN region near the cathode with a length (L_{PC}) of 12 µm was fully etched. Finally, 100-nm SiN_x was deposited by plasma-enhanced chemical vapor deposition for device passivation. Scanning electron microscopy (SEM) images of the multi-channel epi and fabricated devices are shown in Fig. 1(c)-(e).

To experimentally identify T_0, a test structure was used for C-V measurements along with the p-GaN thinning (Fig. 2). When the p-GaN thickness $T > T_0$, at increased reverse biases, the multi-channel is fully depleted first (Fig. 2(a)), producing a C-V characteristic almost unchanged with T. When $T < T_0$, the p-GaN depletion occurs before the full depletion of the 2DEG channels (Fig. 2(b)), leading to a preliminary capacitance drop. The experimental C-V characteristics (Fig. 2(c)) exhibited these behaviors, and the T_0 was extracted to be 80-100 nm.

The multi-channel SBD without a p-GaN termination or p-GaN RESURF was also fabricated as a reference sample. For all these three types of SBDs, the anode-to-cathode distance (L_{AC}) ranges from 48 to 148 µm with a step of 25 µm.

III. Experimental Results

Fig. 3 (a) and (b) show the forward characteristics of the p-GaN-terminated SBDs with L_{AC} of 98, 123, and 148 µm and the p-GaN RESURF SBDs with L_{AC} of 48, 73, 98, and 123 µm. A same turn-on voltage (V_{on}) was extracted to be 0.6 V for all

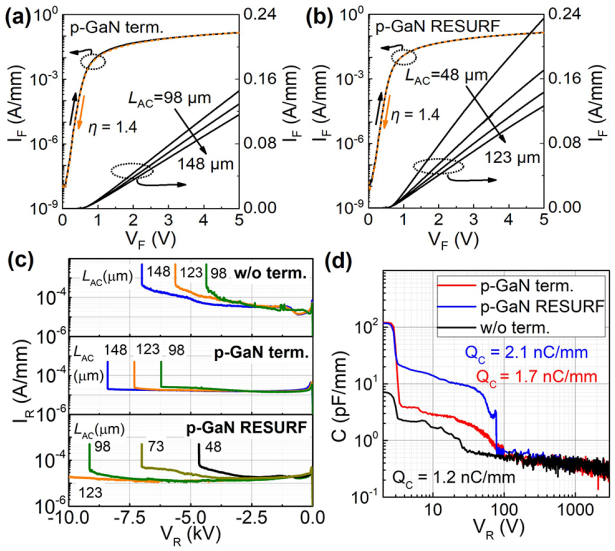

Fig. 3. Forward I-V characteristics of (a) p-GaN-terminated and (b) p-GaN RESURF SBDs with different L_{AC}, in semi-log and linear plots. (c) Reverse I-V characteristics of the SBDs without termination, with p-GaN termination, and with p-GaN RESURF, all with different L_{AC}. Our measurement limit is 10 kV. (d) C-V characteristics of the p-GaN-terminated, p-GaN-RESURF, and non-terminated SBDs with 123 µm L_{AC} at 1 MHz.

SBDs at 1 mA/mm. No hysteresis is observed in the double sweep. The on/off ratio is ~10^7 extracted from the currents at 3 V and 0 V. The Schottky barrier height was extracted to be 0.62 eV and the ideality factor to be 1.4, indicating good-quality contact formed on the etched sidewall. A low on-resistance (R_{on}) of 28.7 and 31 Ω·mm was extracted in the p-GaN RESURF SBDs with 98 and 123 µm L_{AC}, respectively.

Fig. 3(c) shows reverse I-V characteristics of the three types of SBDs with increased L_{AC}. All devices are rinsed in Fluorinert FC-70 in the measurement. With an identical L_{AC} (e.g., 98 µm), the p-GaN RESURF SBD shows a BV about 2-fold higher than that of the SBD without edge termination and about 1.5-fold higher than that of the SBD with p-GaN termination. Despite the non-uniform E-field, an average lateral E-field ($E_{AVE} = BV / L_{AC}$) can be calculated, which is useful for the lateral device design. At a BV of ~5 kV and above, the E_{AVE} of non-terminated SBDs, p-GaN-terminated SBDs, and p-GaN RESURF SBDs are 0.42-0.47 MV/cm, 0.59-0.64 MV/cm, 0.94-1 MV/cm, respectively. This comparison shows the superiority of the p-GaN RESURF structure for E-field management.

The p-GaN RESURF SBD with 98 µm L_{AC} shows a BV of 9.15 kV; the device with 123 µm L_{AC} was measured to 10 kV (our measurement limit) repeatedly without showing any degradation. The leakage current at 10 kV is 1.8×10^{-5} A/mm. Based on the calculated E_{AVE}, the BV of this p-GaN RESURF SBD with 123 µm L_{AC} is projected to be ~11 kV. Note that all the devices fabricated in this work do not show avalanche capability, and their breakdown is catastrophic.

Fig. 3(d) shows the C-V characteristics of p-GaN-terminated, p-GaN RESURF, and non-terminated SBDs with 123 µm L_{AC} measured up to 3 kV. The total capacitive charge (Q_C) was extracted through C-V integration to 3 kV, being 1.7 nC/mm for the p-GaN-terminated SBD and 2.1 nC/mm for the p-GaN RESURF SBD. The higher Q_C in the latter device comes from

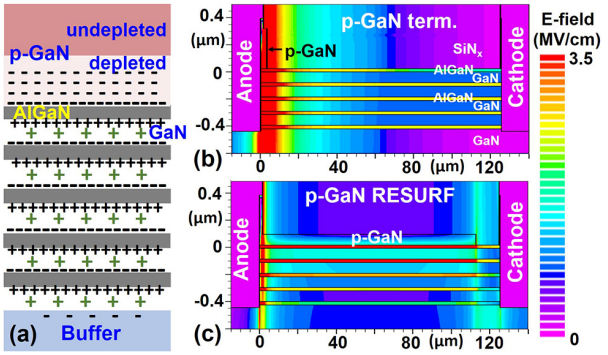

Fig. 4. (a) Schematics of charges in the multi-channel p-GaN RESURF SBD at high V_R. Simulated E-field distribution in (b) p-GaN-terminated and (c) p-GaN RESURF SBDs at V_R = 10 kV.

the higher capacitance at the reverse bias (V_R) below 75 V when the p-GaN RESURF region is not fully depleted and adds a parallel capacitance. In comparison, the p-GaN termination has a very short length, and its capacitance is much smaller.

After the RESURF p-GaN is depleted, C-V characteristics of the two SBDs are almost identical, both reflecting the depletion of multi-channel and buffer regions. The capacitive energy [$E_C = \int Q_C(V_R)dV_R$] is a critical metric of power diodes related to switching losses. Despite a higher Q_C in the RESURF SBD, its E_C up to 3 kV (1.6 μJ/mm) is only 5% higher than that of the p-GaN-terminated SBD. This is because the higher Q_C in the RESURF SBD is mostly present at low V_R.

TCAD simulations were performed in Silvaco Atlas to probe the E-field modulation by the RESURF structure. Fig. 4(a) shows the charge schematic in the RESURF multi-channel at high V_R. Each heterostructure has polarization charges at heterogenous interfaces [8]. Donors are considered to account the unintentional doping in AlGaN/GaN. The p-GaN depletion charge balances the net charges in the multi-channel region. The simulation model is based on [9], [14], and the setup of polarization charges and depleted donor charges are tuned via calibrations with device I-V and C-V characteristics.

Fig. 4(b) and (c) show the simulated E-field distribution in a p-GaN-terminated SBD and a RESURF SBD with 123 μm L_{AC} at 10 kV. The RESURF SBD shows a spreading E-field in the lateral "drift" region and a relaxed E-field crowding near the anode, which explains the higher E_{AVE}. The peak E-field is over 5 MV/cm in the simulated p-GaN-terminated SBD and 3.5 MV/cm in the simulated p-GaN-RESURF SBD, further proving the effectiveness of E-field management.

Note that our RESURF multi-channel SBD is not an ideal PSJ device, which requires an exact charge balance in each heterostructure [8]. Despite the use of a thick i-GaN in each heterostructure, which allows balanced polarization charges according to band theories, our experimental devices exhibited net charges in the multi-channel, probably due to additional donors in AlGaN/GaN. Theoretically speaking, if an ideal PSJ is realized in a multi-channel device, no RESURF structure is needed, and the p-GaN-terminated device should show an equally high E_{AVE}. Actually, the RESURF multi-channel structure proposed in this work shows an effective design for an unbalanced PSJ device, while the ideal multi-channel PSJ device may be very difficult to realize experimentally.

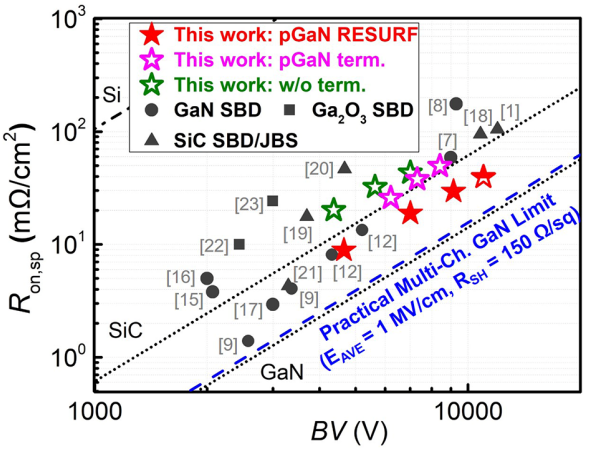

Fig. 5. The differential $R_{ON,SP}$ *v.s.* BV benchmark for our SBDs and the state-of-the-art GaN, SiC, and Ga_2O_3 HV SBDs. The Si, SiC, GaN bulk limits and the multi-channel lateral AlGaN/GaN limit are also plotted.

Fig. 5 benchmarks the $R_{ON,SP}$ *v.s.* BV of our GaN SBDs with the state-of-the-art HV (BV > 2 kV) GaN SBDs [7]–[9], [12], [15]–[17], SiC JBS/SBDs [1], [18]–[21], and Ga_2O_3 SBDs [22], [23]. A contact finger length of 3 μm [24] was added to L_{AC}+L_A in $R_{ON,SP}$ calculation. Our 4.6-10 kV multi-channel RESURF SBDs show a Baliga's FOM ($BV^2/R_{ON,SP}$) of over 2.8 GW/cm^2, which is the highest among all reported 5-kV+ SBDs and well exceeds the 1-D SiC unipolar limit. The practical performance limit of the AlGaN/GaN RESURF multi-channel devices [$R_{on,sp} = BV^2/(q\mu_{2DEG}n_{2DEG}E_{AVE}^2)$] was found to reach the vertical GaN limit using E_{AVE} = 1 MV/cm and R_{SH} = 150 Ω/sq. Note that this practical limit is lower than the theoretical limit of an ideal GaN multi-channel PSJ device.

In addition to 2.5-fold lower differential $R_{ON,SP}$, our 10-kV GaN SBD has a V_{ON} (0.6 V) lower than that of 10-kV SiC JBS diode (>1 V [18], [19]), suggesting a lower forward voltage (V_F). Assuming an 80 mA/mm forward current, the switching FOM (V_F·Q_C) of a 10-kV, 0.3-A GaN multi-channel RESURF SBD is projected to be 15.7 nC·V, which is even lower than that of a commercial 3.3-kV, 0.3-A SiC SBD (30.8 nC·V) [25] (no Q_C data available for higher-voltage SiC SBDs).

The cost of 4-inch GaN-on-sapphire wafer is at least 2~3-fold lower than 4-inch SiC wafer [26]. Together with a much smaller die size, the material cost of our GaN SBDs is expected to be much lower than similarly-rated SiC SBDs. The processing cost of lateral GaN devices is also expected to be lower than SiC.

IV. Summary

We demonstrate multi-channel AlGaN/GaN SBDs with a $R_{ON,SP}$ of 39 mΩ·cm^2 and a BV over 10 kV, by using a novel p-GaN RESURF structure for E-field management. This work reports the highest BV in GaN devices to date. In comparison with 10-kV SiC JBS diodes, our GaN SBDs have a 2.5-fold lower differential $R_{ON,SP}$, a lower V_{ON}, a much smaller projected V_F·Q_C FOM, and a much lower projected cost. These results show the great potential of GaN HV power devices.

References

[1] J. B. Casady, V. Pala, D. J. Lichtenwalner, E. V. Brunt, B. Hull, G. Wang, J. Richmond, S. T. Allen, D. Grider, and J. W. Palmour, "New

Generation 10kV SiC Power MOSFET and Diodes for Industrial Applications," in *Proceedings of PCIM Europe 2015; International Exhibition and Conference for Power Electronics, Intelligent Motion, Renewable Energy and Energy Management*, May 2015, pp. 1–8.

[2] H. Ohta, K. Hayashi, F. Horikiri, M. Yoshino, T. Nakamura, and T. Mishima, "5.0 kV breakdown-voltage vertical GaN p–n junction diodes," *Jpn. J. Appl. Phys.*, vol. 57, no. 4S, p. 04FG09, Feb. 2018, doi: 10.7567/JJAP.57.04FG09.

[3] T. Hayashida, T. Nanjo, A. Furukawa, and M. Yamamuka, "Vertical GaN merged PiN Schottky diode with a breakdown voltage of 2 kV," *Appl. Phys. Express*, vol. 10, no. 6, p. 061003, May 2017, doi: 10.7567/APEX.10.061003.

[4] Y. Zhang and T. Palacios, "(Ultra)Wide-Bandgap Vertical Power FinFETs," *IEEE Trans. Electron Devices*, vol. 67, no. 10, pp. 3960–3971, Oct. 2020, doi: 10.1109/TED.2020.3002880.

[5] T. Oka, "Recent development of vertical GaN power devices," *Jpn. J. Appl. Phys.*, vol. 58, no. SB, p. SB0805, Apr. 2019, doi: 10.7567/1347-4065/ab02e7.

[6] J. Liu, M. Xiao, Y. Zhang, S. Pidaparthi, H. Cui, A. Edwards, L. Baubutr, W. Meier, C. Coles, and C. Drowley, "1.2 kV Vertical GaN Fin JFETs with Robust Avalanche and Fast Switching Capabilities," in *2020 IEEE International Electron Devices Meeting (IEDM)*, Dec. 2020, p. 23.2.1-23.2.4, doi: 10.1109/IEDM13553.2020.9372048.

[7] A. Colón, E. A. Douglas, A. J. Pope, B. A. Klein, C. A. Stephenson, M. S. Van Heukelom, A. Tauke-Pedretti, and A. G. Baca, "Demonstration of a 9 kV reverse breakdown and 59 mΩ-cm2 specific on-resistance AlGaN/GaN Schottky barrier diode," *Solid-State Electron.*, vol. 151, pp. 47–51, Jan. 2019, doi: 10.1016/j.sse.2018.10.009.

[8] H. Ishida, D. Shibata, H. Matsuo, M. Yanagihara, Y. Uemoto, T. Ueda, T. Tanaka, and D. Ueda, "GaN-based Natural Super Junction Diodes with Multi-channel Structures," in *2008 IEEE International Electron Devices Meeting (IEDM)*, Dec. 2008, doi: 10.1109/IEDM.2008.4796636.

[9] M. Xiao, Y. Ma, K. Cheng, K. Liu, A. Xie, E. Beam, Y. Cao, and Y. Zhang, "3.3 kV Multi-Channel AlGaN/GaN Schottky Barrier Diodes With P-GaN Termination," *IEEE Electron Device Lett.*, vol. 41, no. 8, pp. 1177–1180, Aug. 2020, doi: 10.1109/LED.2020.3005934.

[10] J. Ma, C. Erine, M. Zhu, N. Luca, P. Xiang, K. Cheng, and E. Matioli, "1200 V Multi-Channel Power Devices with 2.8 Ω·mm ON-Resistance," in *2019 IEEE International Electron Devices Meeting (IEDM)*, Dec. 2019, p. 4.1.1-4.1.4, doi: 10.1109/IEDM19573.2019.8993536.

[11] Y. Zhang, A. Zubair, Z. Liu, M. Xiao, J. Perozek, Y. Ma, and T. Palacios, "GaN FinFETs and trigate devices for power and RF applications: review and perspective," *Semicond. Sci. Technol.*, vol. 36, no. 5, p. 054001, Mar. 2021, doi: 10.1088/1361-6641/abde17.

[12] M. Xiao, Y. Ma, Z. Du, X. Yan, R. Zhang, K. Cheng, K. Liu, A. Xie, E. Beam, Y. Cao, H. Wang, and Y. Zhang, "5 kV Multi-Channel AlGaN/GaN Power Schottky Barrier Diodes with Junction-Fin-Anode," in *2020 IEEE International Electron Devices Meeting (IEDM)*, Dec. 2020, p. 5.4.1-5.4.4, doi: 10.1109/IEDM13553.2020.9372025.

[13] S.-W. Han, J. Song, S. H. Yoo, Z. Ma, R. M. Lavelle, D. W. Snyder, J. M. Redwing, T. N. Jackson, and R. Chu, "Experimental Demonstration of Charge- Balanced GaN Super-Heterojunction Schottky Barrier Diode Capable of 2.8 kV Switching," *IEEE Electron Device Lett.*, vol. 41, no. 12, pp. 1758–1761, Dec. 2020, doi: 10.1109/LED.2020.3029619.

[14] Y. Zhang, M. Sun, Z. Liu, D. Piedra, H. S. Lee, F. Gao, T. Fujishima, and T. Palacios, "Electrothermal Simulation and Thermal Performance Study of GaN Vertical and Lateral Power Transistors," *IEEE Trans. Electron Devices*, vol. 60, no. 7, pp. 2224–2230, Jul. 2013, doi: 10.1109/TED.2013.2261072.

[15] C. W. Tsou, K. P. Wei, Y. W. Lian, and S. S. H. Hsu, "2.07-kV AlGaN/GaN Schottky Barrier Diodes on Silicon With High Baliga's Figure-of-Merit," *IEEE Electron Device Lett.*, vol. 37, no. 1, pp. 70–73, Jan. 2016, doi: 10.1109/LED.2015.2499267.

[16] J. Ma and E. Matioli, "2 kV slanted tri-gate GaN-on-Si Schottky barrier diodes with ultra-low leakage current," *Appl. Phys. Lett.*, vol. 112, no. 5, p. 052101, Jan. 2018, doi: 10.1063/1.5012866.

[17] T. Zhang, J. Zhang, H. Zhou, Y. Wang, T. Chen, K. Zhang, Y. Zhang, K. Dang, Z. Bian, J. Zhang, S. Xu, X. Duan, J. Ning, and Y. Hao, "A > 3 kV/2.94 mΩcm2 and Low Leakage Current With Low Turn-On Voltage Lateral GaN Schottky Barrier Diode on Silicon Substrate With Anode Engineering Technique," *IEEE Electron Device Lett.*, vol. 40, no. 10, pp. 1583–1586, Oct. 2019, doi: 10.1109/LED.2019.2933314.

[18] J. Lynch, N. Yun, and W. Sung, "Design Considerations for High Voltage SiC Power Devices: An Experimental Investigation into Channel Pinching of 10kV SiC Junction Barrier Schottky (JBS) Diodes," in *2019 31st International Symposium on Power Semiconductor Devices and ICs (ISPSD)*, May 2019, pp. 223–226, doi: 10.1109/ISPSD.2019.8757593.

[19] J. Millán, P. Friedrichs, A. Mihaila, V. Soler, J. Rebollo, V. Banu, and P. Godignon, "High-voltage SiC devices: Diodes and MOSFETs," in *2015 International Semiconductor Conference (CAS)*, Oct. 2015, pp. 11–18, doi: 10.1109/SMICND.2015.7355148.

[20] J. Schoeck, J. Buettner, M. Rommel, T. Erlbacher, and A. J. Bauer, "4.5 kV SiC Junction Barrier Schottky Diodes with Low Leakage Current and High Forward Current Density," *Mater. Sci. Forum*, vol. 897, pp. 427–430, 2017, doi: 10.4028/www.scientific.net/MSF.897.427.

[21] R. Ghandi, A. Bolotnikov, D. Lilienfeld, S. Kennerly, and R. Ravisekhar, "3kV SiC Charge-Balanced Diodes Breaking Unipolar Limit," in *2019 31st International Symposium on Power Semiconductor Devices and ICs (ISPSD)*, May 2019, pp. 179–182, doi: 10.1109/ISPSD.2019.8757568.

[22] W. Li, K. Nomoto, Z. Hu, D. Jena, and H. G. Xing, "Field-Plated Ga_2O_3 Trench Schottky Barrier Diodes With a $BV^2/R_{ON,SP}$ of up to 0.95 GW/cm^2," *IEEE Electron Device Lett.*, vol. 41, no. 1, pp. 107–110, Jan. 2020, doi: 10.1109/LED.2019.2953559.

[23] Z. Hu, H. Zhou, Q. Feng, J. Zhang, C. Zhang, K. Dang, Y. Cai, Z. Feng, Y. Gao, X. Kang, and Y. Hao, "Field-Plated Lateral β-Ga_2O_3 Schottky Barrier Diode With High Reverse Blocking Voltage of More Than 3 kV and High DC Power Figure-of-Merit of 500 MW/cm^2," *IEEE Electron Device Lett.*, vol. 39, no. 10, pp. 1564–1567, Oct. 2018, doi: 10.1109/LED.2018.2868444.

[24] R. Zhang, J. P. Kozak, M. Xiao, J. Liu, and Y. Zhang, "Surge-Energy and Overvoltage Ruggedness of P-Gate GaN HEMTs," *IEEE Trans. Power Electron.*, vol. 35, no. 12, pp. 13409–13419, Dec. 2020, doi: 10.1109/TPEL.2020.2993982.

[25] "GAP3SLT33-214 GeneSiC Semiconductor | Discrete Semiconductor Products." [online available] https://www.digikey.com/en/products/detail/genesic-semiconductor/GAP3SLT33-214/3904847?s=N4IgjCBcoLQBxVAYygMwIYBsDOBTANCAPZQDa4ATACwUgC6Avg4bZOQOICCACgMwDKAGQAqvXjApgq9BkA (accessed Mar. 22, 2021).

[26] Y. Zhang, A. Dadgar, and T. Palacios, "Gallium nitride vertical power devices on foreign substrates: a review and outlook," *J. Phys. Appl. Phys.*, vol. 51, no. 27, p. 273001, 2018, doi: 10.1088/1361-6463/aac8aa.